Computational Study of Bridge Splitting, Aryl Halide Oxidative Addition to Pt^{II}, and Reductive Elimination from Pt^{IV}: Route to Pincer-Pt^{II} Reagents with Chemical and Biological Applications

Allan J. Canty,*[a] Alireza Ariafard,[a] and Gerard van Koten[b]

Abstract: Density functional theory computation indicates that bridge splitting of $[Pt^{II}R_2(\mu\text{-}SEt_2)]_2$ proceeds by partial dissociation to form $R_2Pt^a(\mu\text{-}SEt_2)Pt^bR_2(SEt_2)$, followed by coordination of N-donor bromoarenes (L-Br) at Pt^a leading to release of $Pt^bR_2(SEt_2)$, which reacts with a second molecule of L-Br, providing two molecules of $PtR_2(SEt_2)$(L-Br-*N*). For R = 4-tolyl (Tol), L-Br = 2,6-$(pzCH_2)_2C_6H_3Br$ (pz = pyrazol-1-yl) and 2,6-$(Me_2NCH_2)_2C_6H_3Br$, subsequent oxidative addition assisted by intramolecular N-donor coordination via $Pt^{II}Tol_2$(L-*N,Br*) and reductive elimination from Pt^{IV} intermediates gives *mer*-Pt^{II}(L-*N,C,N*)Br and Tol_2. The strong σ-donor influence of Tol groups results in subtle differences in oxidative addition mechanisms when compared with related aryl halide oxidative addition to palladium(II) centres. For R = Me and L-Br = 2,6-$(pzCH_2)_2C_6H_3Br$, a stable Pt^{IV} product, *fac*-$Pt^{IV}Me_2${2,6-$(pzCH_2)_2C_6H_3$-*N,C,N*}Br is predicted, as reported experimentally, acting as a model for undetected and unstable $Pt^{IV}Tol_2${L-*N,C,N*}Br undergoing facile Tol_2 reductive elimination. The mechanisms reported herein enable the synthesis of Pt^{II} pincer reagents with applications in materials and bio-organometallic chemistry.

Introduction

Organometallic complexes containing a meridionally oriented tridentate ligand in the fragment M(E,E′,E″), where at least one of the donor atoms (E, E′, E″) is carbon, constitute a significant class of "pincer" systems widely studied for their applications in metal-mediated synthesis, catalysis, materials chemistry and applications in biological chemistry.[1] The synthesis of platinum (II) complexes **I** (Scheme 1a)[2] plays a key role in the development of Pt(N,C,N) chemistry. The synthetic method, using $[PtTol_2(SEt_2)]_2$ (Tol = 4-tolyl; **1**),[3] illustrated in Scheme 1b for the model bromoarene 2,6-$(Me_2NCH_2)_2C_6H_3Br$, is applicable for a wide range of Z. Iodoarenes react similarly, but have been less utilised.[5] High isolated yields are obtained from reactions in refluxing benzene or toluene (78–96%),[2,4] except for Z = $CH_2NHCH(iso\text{-}Pr)(CO_2Me)$ (59%).[4a]

This procedure enables the synthesis and subsequent chemical transformations of complexes obtained from bromoarenes containing groups Z that are not appropriate for other methods, for example, by lithiation of halogenoarenes. Reagents I and derivatives have been utilised for studies of fundamental chemistry and applications,[2,4,6] for example, synthesis of coordination polymers;[4e,f] studies of multimetal systems[4c,5,6d,e,k] including nanosize complexes (in which Z are

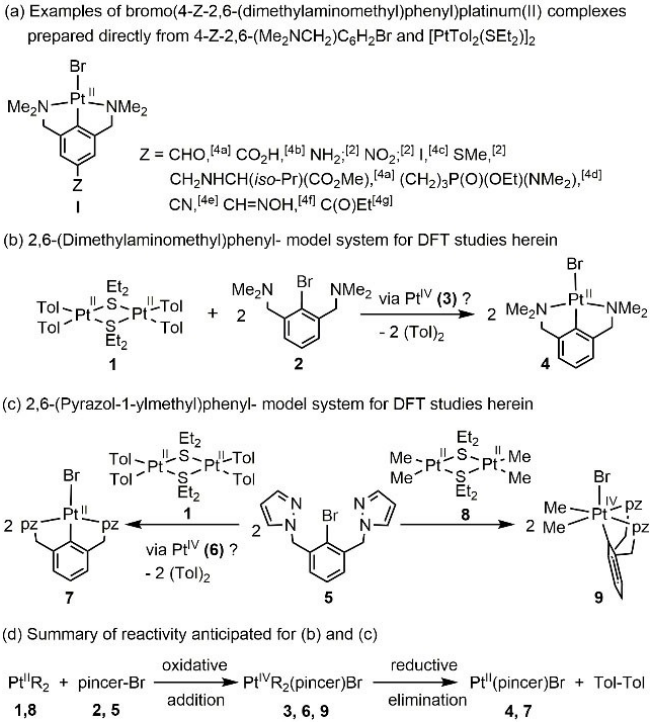

Scheme 1. a) Platinum(II) reagents of wide applicability in studies of pincer chemistry, b) model system for computational study of mechanism reported herein, c) model system for a related pyrazol-1-yl- pincer system, and d) summary of reactivity for (b) and (c).

[a] *Prof. A. J. Canty, Prof. A. Ariafard*
School of Natural Sciences – Chemistry
University of Tasmania
Private Bag 75, Hobart, Tasmania 7001 (Australia)
E-mail: Allan.Canty@utas.edu.au

[b] *Prof. G. van Koten*
Organic Chemistry and Catalysis
Faculty of Science, Utrecht University
Universiteitsweg 99, 3584CG Utrecht (The Netherlands)

Supporting information for this article is available on the WWW under https://doi.org/10.1002/chem.202102687

groups on a dendrimer surface) retained on nanofiltration membranes in a reactor;[5a] electrochemical studies;[5b,6e,g,k] studies of electronic structure including computational studies of Nonlinear optical (NLO) and luminescent properties of stilbenoid complexes with application in an OLED device,[6f,g] electronic properties of organometallic benzylidene anilines,[6l] and orbital examination of π-delocalisation involving the Pt^{II} centre;[6m] bio-organometallic chemistry[4a,d,g,6b–d,g,j,l] including peptide labels containing covalently bonded Pt^{II} centres as diagnostic biomarkers and reversible biosensors for SO_2;[4a,6b] attachment of pincer complexes to carbohydrates,[6i] polypeptides and the protein cutinase;[4d,6j] and post-modification of Tamoxifen to provide candidates for anticancer screening;[4g]

Although the synthetic method continues to be of significant value,[4g] the mechanism has not been established. Oxidative addition of the bromarene to give a Pt^{IV} intermediate followed by reductive elimination is considered to be feasible, in view of related oxidative addition of N-donor bromoarenes to Pt^{II} to form isolated *fac*-Pt^{IV}(N,C,N) complexes,[7] for example, **9** formed in benzene at reflux (Scheme 1c).[7a] Complex **9** has been characterised by X-ray crystallography,[7b] together with the 3,5-dimethylpyrazol-1-yl- analogue of the Pt^{II} complex **7** obtained when $[PtTol_2(SEt_2)]_2$ (**1**) is used as the Pt^{II} reagent.[7b] The similarity of the reaction of Scheme 1b (**1** + **2**→**4**) and c (**1** + **5**→**7**) yielding *mer*-Pt^{II}(N,C,N) moieties, together with isolation of the *fac*-Pt^{IV}(N,C,N) complex **9**, provide support for the possibility of an oxidative addition-reductive elimination sequence for the synthesis of reagents **I**. Isolated yields significantly >50% for syntheses of **I**, Pt^{II} complex **7** (73%) and Pt^{IV} complex **9** (74%) indicate that both Pt^{II} centres in the reagents undergo reaction. We anticipated that reactivity can be summarised as in Scheme 1d.

We have undertaken a computational study of the reactivity shown in Schemes 1b and c, where Scheme 1c is considered as the "benchmark" in view of the experimental dependence on $[PtR_2(SEt_2)]_2$ (R = Me, Tol), involving the formation of isolated Pt^{IV} (R = Me) and Pt^{II} (R = Tol) products. In addition, there are few reports of oxidative addition of aryl-halogen bonds to Pt^{II}, all involving presence of a donor capable of providing intramolecular assistance.[8] These two systems also provide opportunities for examination of mechanism for bridge splitting of dimers, in particular for widely used $[PtR_2(SR'_2)]_2$ reagents.

Whitehurst and Gaunt reported in 2020 the first oxidative addition of halogenoarenes at palladium(II) centres.[9] This procedure gives isolable *mer*-Pd^{IV}(O,C,O) complexes, where the pincer group is $[2,6\text{-}(O_2C)_2C_6H_3]^-$.[9] Our computational study of this system indicates that, after deprotonation of one carboxylic acid substituent of an iodoarene, the precursor for oxidative addition has square-planar geometry formed by a $[C,N]^-$ chelate and an $[O,I]^-$ chelate, Pd^{II}(C~N)(O~I).[10] This report, and a similar study of a related Gaunt system,[11] provided guidance for the present investigation, leading to the interesting discovery of subtle configuration differences in concerted oxidative addition processes, see below (Scheme 2).

Experimental Section

Gaussian 16[12] was used at the B3LYP level of density functional theory (DFT) for geometry optimisation.[13] The Stuttgart/Dresden ECP (SDD) was used to describe Pt,[14] and the 6-31G(d) basis set was used for other atoms to form basis set BS1. Computation was carried out for the experimentally employed solvent benzene utilising the IEFPCM (SCRF) model. To further refine energies obtained from the B3LYP/BS1 calculations, we carried out single-point energy calculations for all structures at the M062-X level[15] incorporating Grimme's D3 computation to account more completely for dispersion.[16] These calculations employed a larger basis set (BS2) utilising the quadrupole-ξ valence polarised def2-QZVP[17] basis set on Pt along with the corresponding ECP and the 6-311 + G(2d,p) basis set on other atoms. All thermodynamic data were calculated at the standard state (298.15 K and 1 atm). To estimate the corresponding Gibbs free energies in benzene, entropy corrections were calculated at the M06/BS1 level and added to the single point potential energies, together with additional corrections for compression of 1 mol of an ideal gas from 1 atm to the 1 M solution phase standard state (1.89 kcal mol^{-1}).[18] Natural bond orbital (NBO) computation utilised NBO7.[19]

Transition structures contained one imaginary frequency, exhibiting atom displacements consistent with the anticipated reaction pathway. The nature of transition structures was confirmed from potential energy surface scans. Intrinsic reaction coordinate (IRC) calculations confirm all transition structures for the key steps of oxidative addition and reductive elimination. For the key step of reductive elimination from Pt^{IV}, calculation of $\Delta G^{\ddagger}$ for reaction at the temperature used experimentally for the reaction (80.1 °C for benzene) show minimal change from that computed at 298.15 K, for example 41.2 kcal mol^{-1} for Me–Me coupling in Figure 1b becomes 39.5 kcal mol^{-1} at 80.1°. We examined the effect of M06 in place of B3LYP for structure determination on the energies of the three key reductive elimination barriers, finding minor changes: **TS-19/22** $\Delta G^{\ddagger}$ 41.2 (Figure 1b) to 39.7 kcal mol^{-1}, **TS-3/37** 24.9 (Figure 2b, below) to 25.0 kcal mol^{-1}, and **TS-6/F** 29.2 (Figure S1 in the Supporting Information) to 27.8 kcal mol^{-1}.

Results and Discussion

We anticipated that formation of a mononuclear square-planar precursor from $[PtR_2(SEt_2)]_2$ (**1**,**8**) would require a bridge-splitting reaction. Consistent with this expectation, we found that potential energy scans for direct interaction of a nitrogen donor of the reagents with dimers **1** or **8** did not support formation of an associative transition state. However, scans do indicate that partial opening of the dimers followed by interaction with **2** or **5** can lead to formation of a complex, and a subsequent pathway to completion of bridge splitting. Computational studies of the reactivity of $2,6\text{-}(pzCH_2)_2C_6H_3Br$ are presented first in view of the experimental characterisation of both Pt^{II} and Pt^{IV} products (Scheme 1c).

Reaction of $[Pt^{II}Me_2(SEt_2)]_2$ (8) with $2,6\text{-}(pzCH_2)_2C_6H_3Br$ (5)

Potential energy scans, including a Pt···Pt scan linking **11** and **12**, and a dihedral angle scan for (Pt-(μ-S)-Pt-$C_{Me\ "bridge"}$) from **12** back to **8**, led to detection of transition state **TS-8/11** and the reaction profile **8**→**12** for partial bridge splitting (Figure 1a).

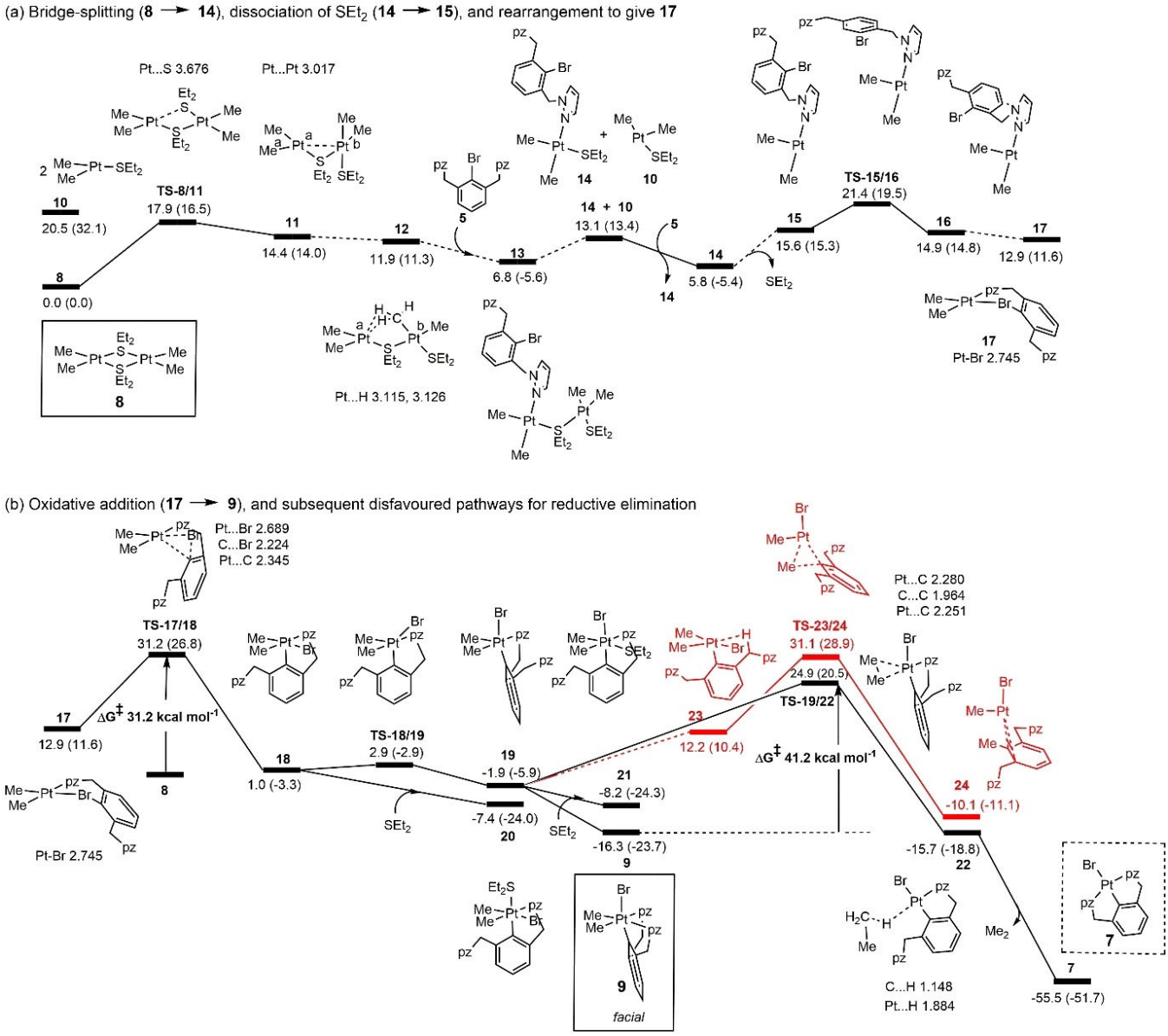

Figure 1. Energy profile for the reaction of $[PtMe_2(SEt_2)]_2$ (**8**) with 2,6-$(pzCH_2)_2C_6H_3Br$ (**5**) to give the isolated Pt^{IV} complex **9**. a) initial steps to give intermediate **17** and b) oxidative addition to give experimentally obtained *facial* **9** (in box). The unfavourable reactivity for reductive elimination to give experimentally unobserved **7** (in dotted box) is also shown. Selected interatomic distances [Å] and energies ΔG (ΔH) [kcal mol^{-1}] referenced to **8** are shown.

Structure **11** exhibits a Pt^a···Pt^b distance (3.017 Å) that is shorter than the sum of van der Waals radii (3.44 Å).[20] A weak Pt^a···Pt^b interaction is indicated by a Wiberg bond index value of 0.108, in contrast to 0.013 for **8** and 0.011 for **12** (NBO calculation). The interaction may be viewed as donation from the four-coordinate Pt^b centre to the three-coordinate Pt^a centre, consistent with computation of 21.05 kcal mol^{-1} for the second-order perturbation energy (E^2) for interaction between the Pd^b d_{z^2} orbital and the Pt^a-C^a σ* orbital. Structure **11** undergoes a facile rearrangement to give **12**. Complex **12** exhibits C–H agostic interactions. Complex **12** interacts with reagent **5** to give complex **13**. A scan for removal of **5** from **13**, by increasing the Pt–N distance, did not reveal a transition state for formation of **13** from **12** and **5**, but did result in separated **5** and **12**.

The bridge-splitting process is completed on dissociation of $PtMe_2(SEt_2)$ (**10**) from complex **13**, giving **14**, followed by reaction of **10** with reagent **5** to give a second molecule of **14**. A transition state for dissociation of **10** from **13** could not be found, although scans for Pt···S bond cleavage indicate a very late transition state. Scans exhibit a maximum energy at approximately 3.5 Å in the scan, compared with the sum of van der Waals radii (3.27 Å).[20] Following the protocol developed by Hartwig and Hall, $\Delta G^{\ddagger}$ approximated as ΔH,[21] we estimate the Gibbs barrier as about 19.0 kcal mol^{-1}, placing the transition state stationary point at about 25.8 kcal mol^{-1} relative to

$[PtMe_2(SEt_2)]_2$ (**8**). A scan for the loss of SEt_2 from **14** to give **15** is also sigmoidal, so that the transition state stationary point is estimated to be at approximately 26.5 kcal mol^{-1}. The same procedure applied to direct cleavage of $[PtMe_2(SEt_2)]_2$ (**8**) to give $PtMe_2(SEt_2)$ (**10**; Figure 1a) provides an estimate for an intermediate stationary point as at about 32 kcal mol^{-1}. This indicates that a direct fragmentation of **8** to two equivalents of **10** is unlikely.

Structure **15** is able to undergo conformational rearrangement to provide **17**, exhibiting the bromoarene as an [N,Br] bidentate ligand with Pt–Br 2.745 Å, significantly shorter than the sum of van der Waals radii (3.57 Å).[20] Oxidative addition proceeds as shown in Figure 1b, for which the overall reaction rate-limiting transition state (**TS-17/18**) for formation of the Pt^{IV} product **9** from dimer **8** computes as $\Delta G^{\ddagger}$ 31.2 kcal mol^{-1}. The immediate product of oxidative addition (**18**) undergoes facile isomerisation (**TS-18/19**) to form **19**, for which the dangling $-CH_2$pz arm coordinates to give 9. Species formed on coordination of SEt_2 (**20**, **21**) are disfavoured relative to **9**.

Potential pathways for reductive elimination from **9** and from **18**–**21** were explored, and the lowest energy transition states for Me–Me (**TS-19/22**) and Me-pincer coupling (**TS-23/24**, in red) are illustrated in Figure 1b. The lowest barrier, $\Delta G^{\ddagger}$ 41.2 kcal mol^{-1} for Me–Me coupling (**TS-19/17**), is greater than that for the oxidative addition step (TS-17/18, $\Delta G^{\ddagger}$ 31.2 kcal mol^{-1}, accounting for the isolation of **9**. Me-pincer coupling is even less favourable (**TS-23/24**, $\Delta G^{\ddagger}$ 47.4 kcal mol^{-1}).

Analogous computation for oxidative addition to $[PtTol_2(SEt_2)]_2$ (**1**; Scheme 1c) reveals a similar reaction profile, resulting in a $Pt^{IV}Tol_2$ analogue of **9**, but in this case reductive elimination of Tol_2 ($\Delta G^{\ddagger}$ 17.1 kcal mol^{-1}) is less than that for the oxidative addition step ($\Delta G^{\ddagger}$ 28.5 kcal mol^{-1}), consistent with experimentally observed formation of the Pt^{II} product 7 (details in the Supporting Information).

Additional aspects of oxidative addition, the structure of isolated product **9**, and reductive elimination are discussed in later sections.

Reaction of $[Pt^{II}Tol_2(SEt_2)]_2$ (1) with 2,6-$(Me_2NCH_2)_2C_6H_3Br$ (2)

Confidence in the computational procedure obtained from agreement between computation and experimental results for the 2,6-$(pzCH_2)_2C_6H_3Br$ system encouraged us to proceed with examination of the 2,6-$(Me_2NCH_2)_2C_6H_3Br$ system, for which Pt^{IV} species have not been detected experimentally. The reaction profile obtained is shown as Figure 2.

In contrast to the $[PtMe_2(SEt_2)]_2$/2,6-$(pzCH_2)_2C_6H_3Br$ system (Figure 1a), the partial opening of dimer **1** occurs via a single transition state (**TS-1/26**; Figure 2a). A precursor adduct (**27**) and transition state (**TS-27/28**) were identified for the coordination of 2,6-$(Me_2NCH_2)_2C_6H_3Br$ to give **28**. Completion of bridge splitting and departure of SEt_2 to give **30** is followed by conformational changes resulting in formation of **32**, the analogue of **17** in Figure 1a.

Oxidative addition via transition state **TS-32/33** is followed by isomerisation to give **3** (Figure 2b). Reductive elimination of Tol_2 occurs directly from **3** via transition state **TS-3/37**, for which $\Delta G^{\ddagger}$ 24.9 kcal mol^{-1} is essentially identical to that for oxidative addition (**TS-32/33**, 24.3 kcal mol^{-1}), ensuring progression to the very low energy product (**4**) consistent with experimental observation that the Pt^{II} complex **4** is the product of reaction. The barrier computed for reductive elimination of Tol-pincer is *G* 1.7 kcal mol^{-1} higher than that for Tol_2 reductive elimination.

Barriers higher than **TS-3/37** (Tol_2 elimination) were also found for five- and six-coordinate transition states potentially originating from SEt_2 structures **35** and **36**, where the five-coordinate structures contain two dangling $-CH_2NMe_2$ groups. A high energy four-coordinate structure with two dangling $-CH_2NMe_2$ groups was also obtained when a transition state from **33** was modelled (details in the Supporting Information).

In view of the extensive chemistry of the *mer*-Pt^{II}(N,C,N) moiety, exemplified in Scheme 1a, we explored intramolecular isomerisation of **33** to generate the *mer*-Pt^{IV}(N,C,N) configuration. We found a very high energy transition state, $\Delta G^{\ddagger}$ 37.6 kcal mol^{-1} relative to resting state **3**, leading to endergonic formation of $Pt^{IV}Tol_2$(*mer*-N,C,N)Br, ΔG 17.2 kcal mol^{-1} relative to $[PtTol_2(SEt_2)]_2$ (**1**; details in the Supporting Information). Thus, the presence of *mer*-Pt^{IV}(N,C,N) species is discounted.

Aryl halide oxidative addition to palladium(II) and platinum (II)

The results reported here provide an opportunity to compare aryl halide oxidative addition at Pd^{II} and Pt^{II} centres, for which isolation of Pd^{IV} and Pt^{IV} products is currently limited to systems where intramolecular assistance is present.[7–9] Scheme 2a illustrates precursors, transition states and immediately formed products identified by computation for Pd,[10] together with subsequent processes to give isolable **IV**.[9] Scheme 2b shows analogous computation leading to isolable Pt^{IV} complex **9**.

Precursor **17** has Pt–Br computed as 2.745 Å, similar to Pt^{IV}-Br in product **9** (2.619 Å (computation), 2.5764(5) Å (X-ray)),[7b] indicating presence of a significant interaction in **17**, although C–Br is decreased by only about 0.01 Å from the value computed for the free ligand (**5**).[22] The Pt–Br interaction is viewed as a Br→Pt donor interaction rather than a halogen-bond interaction, in view of the minor change in C–Br bond length and the markedly nonlinear C–Br–Pt moiety (118.4°),[23] and a typical d^8 square-planar geometry with four donor groups.

The concerted oxidative addition steps, from directly analogous precursors (**II**, **17**) to immediate products (**III**, **18**), exhibit a subtle difference for **II** and **17**. Oxidative addition for Pd provides a square-pyramidal product with the aryl group in the equatorial position (**III**), but for Pt provides distorted square-pyramidal geometry with the aryl group in the axial position (**18**). Although there are differences in the donor sets, we attribute this difference in geometry for **18** to the strong σ-donor influence of methyl groups in **18** disfavouring a *trans*-C–Pt–C configuration required for the aryl group to be in the

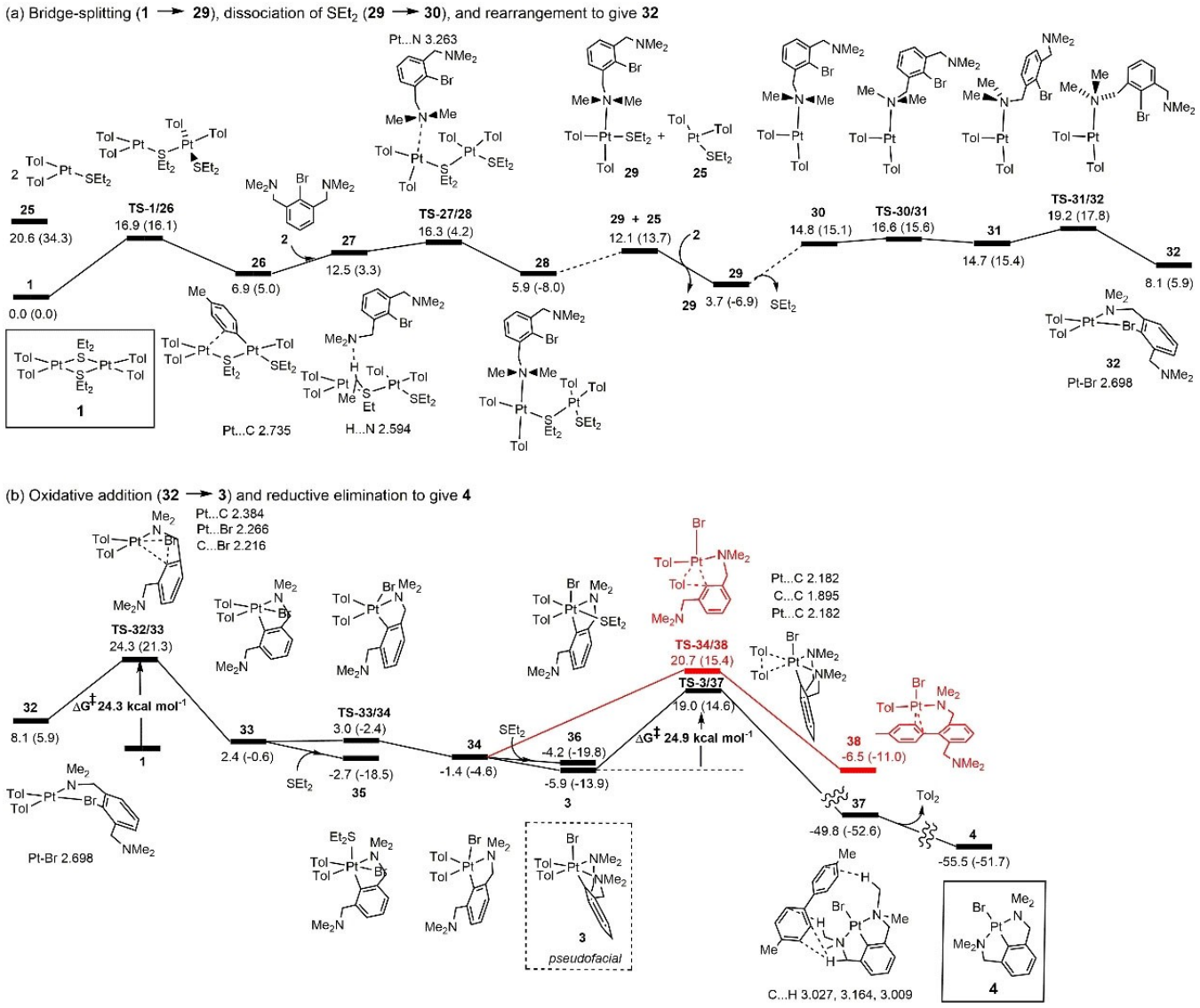

Figure 2. Energy profile for the reaction of $[PtTol_2(SEt_2)]_2$ (**1**) with 2,6-$(Me_2NCH_2)_2C_6H_3Br$ (**2**) to give undetected Pt^{IV} intermediates with Pt^{IV}(C ~ N) moieties (**33**–**36**), followed by reductive elimination from *pseudofacial* **3** (in dotted box) to give experimentally obtained **4** (in box). a) Initial steps to give intermediate **32** and b) oxidative addition to give **3**, together with reductive elimination pathways. Selected interatomic distances [Å] and energies ΔG (ΔH) [kcal mol^{-1}] referenced to **1** are shown.

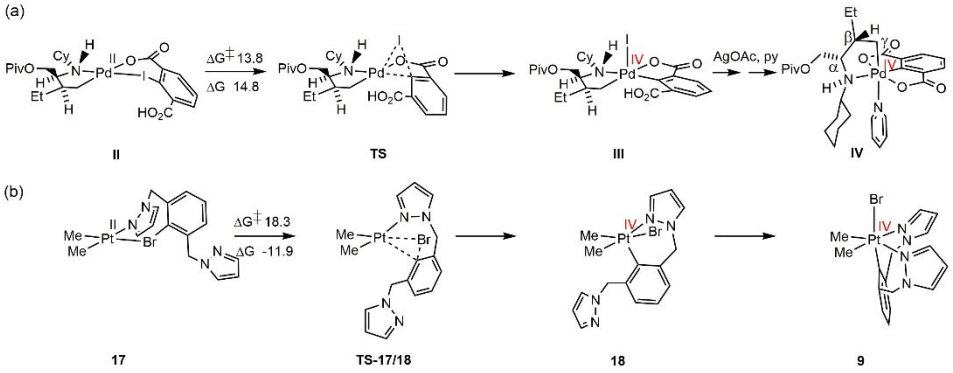

Scheme 2. Computation for precursors, transition states, and initial products for intramolecular assisted oxidative addition for a) palladium(II) to give **III**,[10] followed by subsequent reaction to give **IV**.[9] b) Platinum(II) illustrated for 2,6-$(pzCH_2)_2C_6H_3Br$ to give **18**, followed by intramolecular isomerisation to give **9** (Figure 1b).[7] $\Delta G^{\ddagger}$ and ΔG [kcal mol^{-1}] are referenced to **II** and **17**.

equatorial position. The sequences demonstrate flexibility in concerted aryl halide oxidative addition mechanisms at d^8 M^{II} centres.

Structures of platinum(IV) complexes of terdentate-N,C,N ligands, and reductive elimination

The ligand $[2,6\text{-}(Me_2NCH_2)_2C_6H_3]^-$ has to date not demonstrated an ability to act in a *fac*-Pt^{IV}(N,C,N) manner with angles close to 90°, a result of the steric restraint requiring two five-membered chelate rings, rather than two six-membered chelate rings for $[2,6\text{-}(pzCH_2)_2C_6H_3\text{-}N,C,N]^-$ in complex **9**. However, *pseudofacial-N,C,N* geometries have been documented,[24a] with the smallest N–M–N angle reported to date being 109.35(6)° for Ru^{II}(2,6-$(Me_2NCH_2)_2C_6H_3$-*N,C,N*)(η^4-norbornadiene)(O_3SCF_3-*O*),[24b] in contrast with complex **9** (92.4(2)° (X-ray structure),[7b] 93.8° (computation)). Figure 3 shows computed structures for **3** and **9** with bond angles and distances that characterise the *facial-* and *pseudofacial*-Pt^{IV}(N,C,N) geometries, together with structures of transition states **TS-3/37** for experimentally observed reductive elimination of Tol_2 from **3** and **TS-19/22** for unobserved reductive elimination of Me_2 from **9**.

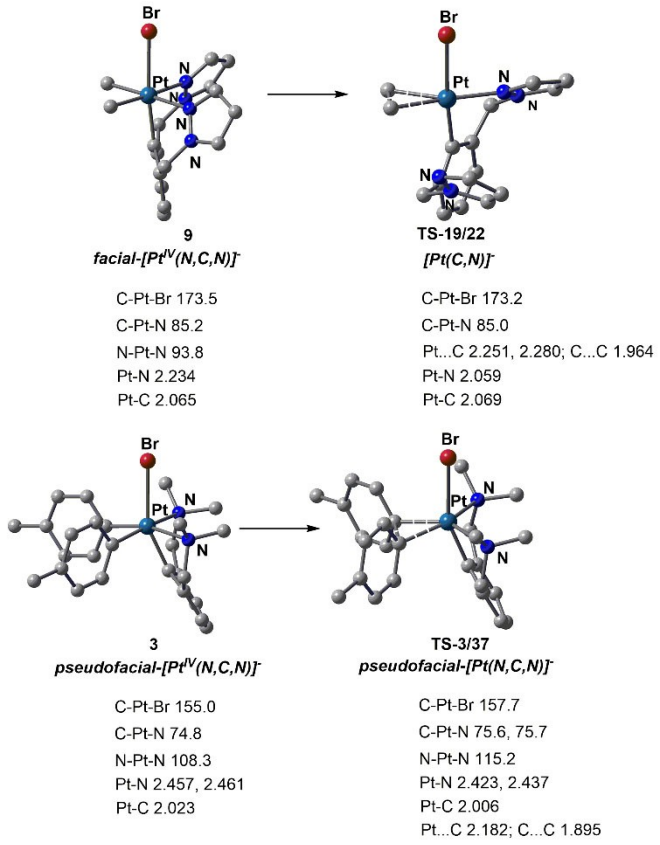

Figure 3. Computed structures for isolated **9**, and the Pt^{IV} resting state **3**, illustrating *facial-* and *pseudofacial*-Pt^{IV}(N,C,N) geometries, respectively, together with structures of transition states for reductive elimination. Hydrogen atoms are omitted for clarity; angles are in degrees and distances in Å.

With regard to structures **9** and **3**, angles at Pt formed by the $[N,C,N]^-$ groups differ by ~5° from 90° in **9**, but differ by ~15° and ~18° in **3**. For both structures, Pt–C and Pt–N bond lengths are very similar to those computed for their related six-coordinate intermediates containing the aryl groups as $[C,N]^-$ donors (**20** and **21** in Figure 1b, **35** and **36** in Figure 2b). The aryl ring in **3** shows some distortion, where C_{ipso} is displaced from the plane of the ring towards the position *trans* to bromide, reflected in a Pt–C_{ipso}···C_{para} angle of 172.4°, compared with 178.4° for **9**. In both systems, the methylene groups of the donor arms are removed from the plane of the arene rings to assist $[N,C,N]^-$ coordination, following a similar trend to Pt-C_{ipso}···C_{para}, with C–C_{ortho}···C_{meta} angles across the rings 165.4° for **3** and 171.9° for the pyrazol-1-yl system in **9**.

The direct analogue of **3** for the pyrazol-1-yl- ligand, *fac*-$Pt^{IV}Tol_2${2-6-$(pzCH_2)_2C_6H_3$-*N,C,N*}Br (**6**), exhibiting an absence of distortion as for **9**, is formed in a more exergonic manner than **3**, $\Delta\Delta G$ 6.2 kcal mol^{-1} (details in the Supporting Information). Although additional considerations apply, this trend is consistent with the proposal that distortion to form the *pseudofacial* configuration is a destabilising factor.

Further insight into the role of distortion is obtained on examination of the structures of key transition states, **TS-19/22** (Figure 3) and the analogous di(tolyl) analogue for the 2,6-$(pzCH_2)_2C_6H_3$Br system (Figure S1), and **TS-3/37** for the 2,6-$(pzCH_2)_2C_6H_3$Br system (Figure 1b). The 2,6-$(pzCH_2)_2C_6H_3$Br system forms a five-coordinate transition state, but the 2,6-$(Me_2NCH_2)_2C_6H_3$Br retains six-coordination with the N–Pt–N angle opposite the reductively eliminating groups increased from that in the precursor complexes, for example from 108.3° in **3** to 115.2° in **TS-3/37** (Figure 3). The increase in this angle is as expected,[26] and also illustrates release of strain present in **3**. Comparing the two ditolyl systems, transformation **3**→**TS-3/37** in Figure 3 and the analogous change for reductive elimination in the 2,6-$(pzCH_2)_2C_6H_3$Br system (**6**→**TS-6/F**, Figure S1), we note that the Gibbs change for this process is 4.3 kcal mol^{-1} lower for **3**, implying that due to the release of distortion for **3** in forming the transition state, this intermediate is more reactive than **6** for reductive elimination.

Carbon-carbon reductive elimination at Pt^{IV} centres generally proceeds from five-coordinate intermediates,[25] although computation indicates a six-coordinate intermediate for vinyl-vinyl coupling[25i] and experimental evidence indicates absence of monodentate ligand dissociation as a preliminary step for some six-coordinate platina(IV)cyclic complexes.[25l] For the 2,6-$(pzCH_2)_2C_6H_3$Br system studied herein, sharing a common coordination geometry for *fac*-$[Pt^{IV}R_2${2,6-$(Me_2NCH_2)_2C_6H_3$-*N,C,N*}Br (R = Me (**9**), R = Tol (**6**, details in the Supporting Information)), Tol–Tol coupling is computed to occur more readily than Me–Me coupling by approximately 6 kcal mol^{-1}. Interestingly, the present systems also illustrate the flexibility in preference for coordination geometry in reductive elimination noted above.[25i,l]

The difference in mechanism for reductive elimination, five-coordination for $C(sp^3)$-$C(sp^3)$ coupling and six-coordination for $C(sp^2)$-$C(sp^2)$ coupling, is closely related to computational results

reported for $Pt^{IV}R_4(PMe_3)_2$: five-coordination for $C(sp^3)$-$C(sp^3)$ (R = Me) and six-coordination for $C(sp^2)$-$C(sp^2)$ (R = vinyl).[25i]

For the *pseudofacial*-Pt^{IV} intermediate, $Pt^{IV}Tol_2${2,6-$(Me_2NCH_2)_2C_6H_3$-*N,C,N*}Br (**3**), we find a preference for direct elimination from the six-coordinate structure via **TS-3/37** (Figure 2b), as found for the analogous complex $Pt^{IV}Tol_2${2,6-$(pzCH_2)_2C_6H_3$-*N,C,N*}Br (6, details in the Supporting Information).

Conclusions

The reaction of $[Pt^{II}Tol_2(SEt_2)]_2$ (1) with 4-Z-2,6-$(Me_2NCH_2)_2C_6H_3$Br to form Pt^{II} complexes such as those illustrated in Scheme 1a proceeds as shown in Scheme 3. Bridge splitting to form **29** [Eq. (1)] is followed by dissociation of SEt_2 from **29** to form **32** [Eq. (2)], oxidative addition to form **3** [Eq. (3)], and reductive elimination from **3** to form **4** [Eq. (4)]. This sequence of reactions utilising $[PtTol_2(SEt_2)]_2$ as a reagent allows the introduction of platinum into complex structures in the late stage of synthesis of Pt(N,C,N) pincer complexes.

The formation of the useful reagents **I** containing the *mer*-Pt^{II}(N,C,N) kernel (Scheme 1a), rather than Pt^{IV} complexes related to that obtained from 2,6-$(pzCH_2)_2C_6H_3$Br (**9**, Scheme 1c), is attributed to two factors. Firstly, there is a lower barrier for Tol-Tol coupling than for Me–Me coupling in Pt^{IV} intermediates: the factor that selects for Pt^{II} (**7**) versus Pt^{IV} (**9**) in the 2,6-$(pzCH_2)_2C_6H_3$Br system (Scheme 1c). Secondly, [4-Z-2,6-$(Me_2NCH_2)_2C_6H_3]^-$ ligands, forming five-membered chelate rings and adopting a *pseudofacial*-Pt^{IV}(N,C,N) configuration, provide Pt^{IV} geometries removed from regular octahedral geometry, and thus less stable. Although both factors are influential, the *dominant* factor is the ease of Tol-Tol coupling, as this factor alone accounts for selectivity in the 2,6-$(pzCH_2)_2C_6H_3$Br system. In addition, coordination of SEt_2 to form regular octahedral *fac*-Pt^{IV}(C,N)(SEt_2) (**35**, **36**; Figure 2b), as alternatives to *pseudofacial*-Pt^{IV}(N,C,N), does not provide additional stability to counter the low barrier for Tol-Tol coupling.

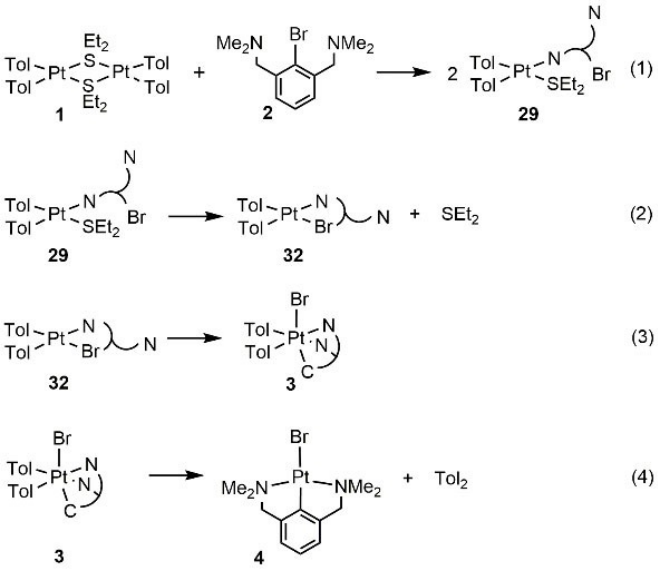

Scheme 3. Sequence of reactions summarising the reaction profile in Scheme 1b, Figure 2a [Eqs (1) and (2)], and Figure 2b [Eqs (3) and (4)].

Computation obtained in exploring the synthetic route to pincer reagents has elucidated interesting insights into mechanisms in organometallic chemistry, in particular:

i) Provided a mechanism for the bridge splitting of widely used dimeric reagents in organoplatinum chemistry, $[PtR_2(SEt_2)]_2$ (**1**, **8**), in which partial cleavage of dimers to form $Pt^aR_2(\mu\text{-}SEt_2)Pt^bR_2(SEt_2)$ (**12** in Figure 1a, **26** in Figure 1b) allows coordination by a ligand at Pt^a and subsequent bridge splitting by cleavage of the Pt^a-(μ-S) bond.

ii) Extended the applicability of the neutral square-planar motif Pd^{II}(*C*~N-*C,N*)(O~I-*O,I*), for intramolecular coordination assisted oxidative addition at Pd^{II},[10,11] to a related motif for platinum, $Pt^{II}R_2$(N~Br-*N,Br*) (R = Me, Tol), and elucidated the effect of σ-donor influence of ligands opposite the Ar-X oxidative addition site in governing the geometry of transition states and products (Scheme 2); and

iii) Allowed a comparison of $C(sp^2)$-$C(sp^2)$ coupling with $C(sp^3)$-$C(sp^3)$ coupling in Pt^{IV} complexes of identical configuration, *fac*-$[PtR_2$(N,C,N)Br], for which Tol-Tol coupling is easier than Me–Me by about 6 kcal mol^{-1}, and exhibiting five- (R = Tol) and six-coordinate (R = Me) transition states.

Acknowledgements

We acknowledge support from the Australian Research Council and the Australian National Computing Infrastructure.

Conflict of Interest

The authors declare no conflict of interest.

Keywords: aryl halides · bridge splitting · coordination modes · oxidative addition · pincer complexes · platinum · reductive elimination

[1] a) C. E. Jones, B. L. Shaw, B. L. Turtle, *J. Chem. Soc. Dalton Trans.* **1974**, 992–999; b) C. J. Moulton, B. L. Shaw, *J. Chem. Soc. Dalton Trans.* **1976**, 1020–1024; c) *Topics in Organometallic Chemistry, Vol. 40: Organometallic Pincer Chemistry* (Eds.: G. van Koten, D. Milstein), Springer, **2013**; d) *Topics in Organometallic Chemistry, Vol. 54: The Privileged Pincer-Metal Platform, Coordination Chemistry and Applications* (Eds.: G. van Koten, R. Gossage), Springer, **2018**; e) *Pincer Compounds: Chemistry and Applications* (Ed.: D. Morales-Morales), Elsevier, **2018**; f) G. van Koten, *Advances in Bioorganometallic Chemistry* (Eds.: T. Hirao, T. Moriuchi), "NCN-Pincer Organometallics in Bioorganometallic Chemistry", Elsevier, **2018**, pp. 113-136; g) M. Albrecht, G. van Koten, *Angew. Chem. Int. Ed.* **2001**, *40*, 3750–3781; *Angew. Chem.* **2001**, *113*, 3866–3898; h) E. Peris, R. H. Crabtree, *Chem. Soc. Rev.* **2018**, *47*, 1959–1968.

[2] M. Q. Slagt, G. Rodríguez, M. M. P. Grutters, R. J. M. Klein Gebbink, W. Klopper, L. W. Jenneskens, M. Lutz, A. L. Spek, G. van Koten, *Chem. Eur. J.* **2004**, *10*, 1331–1344.

[3] a) B. R. Steele, K. Vrieze, *Trans. Met. Chem.* **1977**, *2*, 140–144; b) M. A. Casado Lacabra, A. J. Canty, M. Lutz, J. Patel, A. L. Spek, H. Sun, G. van Koten, *Inorg. Chim. Acta* **2002**, *327*, 15–19.

[4] a) M. Albrecht, G. Rodríguez, J. Schoenmaker, G. van Koten, *Org. Lett.* **2000**, *2*, 3461–3464; b) M. Q. Slagt, R. J. M. Klein Gebbink, M. Lutz, A. L.

Spek, G. van Koten, *J. Chem. Soc. Dalton Trans.* **2002**, 2591–2592; c) G. Rodríguez, M. Albrecht, J. Schoenmaker, A. Ford, M. Lutz, A. L. Spek, G. van Koten, *J. Am. Chem. Soc.* **2002**, *124*, 5127–5138; d) C. A. Kruithof, M. A. Casado, G. Guillena, M. R. Egmond, A. van der Kerk-van Hoof, A. J. R. Heck, R. J. M. Klein Gebbink, G. van Koten, *Chem. Eur. J.* **2005**, *11*, 6869–6877; e) S. Köcher, B. Walfort, A. M. Mills, A. L. Spek, G. P. M. van Klink, G. van Koten, H. Lang, *J. Organomet. Chem.* **2008**, *693*, 1991–1996; f) S. Köcher, M. Lutz, A. L. Spek, B. Walfort, T. Ruffer, G. P. M. van Klink, G. van Koten, H. Lang, *J. Organomet. Chem.* **2008**, *693*, 2244–2250; g) G. D. Batema, T. J. Korstanjie, G. Guillena, G. Rodriguez, M. Lutz, G. P. M. van Klink, R. A. Gossage, G. van Koten, *Molecules* **2021**, *26*,1888–1906.

[5] a) H. P. Dijkstra, C. A. Kruithof, N. Ronde, R. van de Coevering, D. J. Ramón, D. Vogt, G. P. M. van Klink, G. van Koten, *J. Org. Chem.* **2003**, *68*, 675–685; b) S. Köcher, M. Lutz, A. L. Spek, R. Prasad, G. P. M. van Klink, G. van Koten, H. Lang, *Inorg. Chim. Acta* **2006**, *359*, 4454–4462.

[6] a) B. M. J. M. Suijkerbuijk, M. Q. Slagt, R. J. M. Klein Gebbink, M. Lutz, A. L. Spek, G. van Koten, *Tetrahedron Lett.* **2002**, *43*, 6565–6568; b) G. Guillena, G. Rodríguez, M. Albrecht, G. van Koten, *Chem. Eur. J.* **2002**, *8*, 5368–5376; c) G. Guillena, K. M. Halkes, G. Rodríguez, G. D. Batema, G. van Koten, J. P. Kamerling, *Org. Lett.* **2003**, *5*, 2021–2024; d) S.-E. Stiriba, M. Q. Slagt, H. Kautz, R. J. M. Klein Gebbink, R. Thomann, H. Frey, G. van Koten, *Chem. Eur. J.* **2004**, *10*, 1267–1273; e) S. Köcher, G. P. M. van Klink, G. van Koten, H. Lang, *J. Organomet. Chem.* **2006**, *691*, 3319–3324; f) G. D. Batema, K. T. L. van de Westelaken, J. Guerra, M. Lutz, A. L. Spek, C. A. van Walree, C. de Mello Donegá, A. Meijerink, G. P. M. van Klink, G. van Koten, *Eur. J. Inorg. Chem.* **2007**, 1422–1435; g) G. D. Batema, M. Lutz, A. L. Spek, C. A. van Walree, C. de Mello Donegá, A. Meijerink, R. W. A. Havenith, J. Pérez-Moreno, K. Clays, M. Büchel, A. van Dijken, D. L. Bryce, G. P. M. van Klink, G. van Koten, *Organometallics* **2008**, *27*, 1690–1701; h) K. Döring, D. Taher, B. Walfort, M. Lutz, A. L. Spek, G. P. M. Klink, G. van Koten, H. Lang, *Inorg. Chim. Acta* **2008**, *361*, 2731–2739; i) B. Wieczorek, H. P. Dijkstra, M. R. Egmond, R. J. M. Klein Gebbink, G. van Koten, *J. Organomet. Chem.* **2009**, *694*, 812–822; j) L. Rutten, B. Wieczorek, J.-P. B. A. Mannie, C. A. Kruithof, H. P. Dijkstra, M. R. Egmond, M. Lutz, R. J. M. Klein Gebbink, P. Gros, G. van Koten, *Chem. Eur. J.* **2009**, *15*, 4270–4280; k) S. Bonnet, M. A. Siegler, J. H. van Lenthe, M. Lutz, A. L. Spek, G. van Koten, R. J. M. Klein Gebbink, *Eur. J. Inorg. Chem.* **2010**, 4667–4677; l) G. D. Batema, M. Lutz, A. L. Spek, C. A. van Walree, G. P. M. van Klink, G. van Koten, *Dalton Trans.* **2014**, *43*,12200–12209; m) A. J. Canty, A. Ariafard, G. van Koten, *Chem. Eur. J.* **2020**, *26*, 15629–15635.

[7] a) A. J. Canty, R. T. Honeyman, B. W. Skelton, A. H. White, *J. Organomet. Chem.* **1990**, *389*, 277–288; b) A. J. Canty, J. Patel, B. W. Skelton, A. H. White, *J. Organomet. Chem.* **2000**, *599*, 195–199.

[8] a) C. M. Anderson, R. J. Puddephatt, G. Ferguson, A. J. Lough, *J. Chem. Soc. Chem. Commun.* **1989**, 1297–1298; b) C. M. Anderson, M. Crespo, M. C. Jennings, A. J. Lough, G. Ferguson, R. J. Puddephatt, *Organometallics* **1991**, *10*, 2672–2679; c) C. M. Anderson, M. Crespo, G. Ferguson, A. J. Lough, R. J. Puddephatt, *Organometallics* **1992**, *11*, 1177–1181; d) M. C. Crespo, C. Grande, A. Klein, *J. Chem. Soc. Dalton Trans.* **1999**, 1629–1637; e) T. Calvet, M. Crespo, M. Font-Bardía, S. Jansat, M. Martínez, *Organometallics* **2012**, *31*, 4367–4373.

[9] W. G. Whitehurst, M. J. Gaunt, *J. Am. Chem. Soc.* **2020**, *142*, 14169–14177.

[10] A. J. Canty, A. Ariafard, *Organometallics* **2021**, *40*, 1262–1269.

[11] X. Ma, Z. Han, C. Liu, D. Zhang, *Inorg. Chem.* **2020**, *59*, 18295–18304.

[12] M. J. Frisch, G. W. Trucks, H. B. Schlegel, G. E. Scuseria, M. A. Robb, J. R. Cheeseman, G. Scalmani, V. Barone, G. A. Petersson, H. Nakatsuji, X. Li, M. Caricato, A. V. Marenich, J. Bloino, B. G. Janesko, R. Gomperts, B. Mennucci, H. P. Hratchian, J. V. Ortiz, A. F. Izmaylov, J. L. Sonnenberg, D. Williams-Young, F. Ding, F. Lipparini, F. Egidi, J. Goings, B. Peng, A. Petrone, T. Henderson, D. Ranasinghe, V. G. Zakrzewski, J. Gao, N. Rega, G. Zheng, W. Liang, M. Hada, M. Ehara, K. Toyota, R. Fukuda, J. Hasegawa, M. Ishida, T. Nakajima, Y. Honda, O. Kitao, H. Nakai, T. Vreven, K. Throssell, J. A. Montgomery, Jr., J. E. Peralta, F. Ogliaro, M. J. Bearpark, J. J. Heyd, E. N. Brothers, K. N. Kudin, V. N. Staroverov, T. A. Keith, R. Kobayashi, J. Normand, K. Raghavachari, A. P. Rendell, J. C. Burant, S. S. Iyengar, J. Tomasi, M. Cossi, J. M. Millam, M. Klene, C. Adamo, R. Cammi, J. W. Ochterski, R. L. Martin, K. Morokuma, O. Farkas, J. B. Foresman, D. J. Fox, *Gaussian 16Revision B.01*; Gaussian, Inc., Wallingford CT, **2016**.

[13] a) C. Lee, W. Yang, R. G. Parr, *Phys. Rev. B* **1988**, *37*, 785–789; b) B. Miehlich, A. Savin, H. Stoll, H. Preuss, *Chem. Phys. Lett.* **1989**, *157*, 200–206; c) A. D. Becke, *J. Chem. Phys.* **1993**, *98*, 5648–5652; d) P. J. Stephens, F. J. Devlin, C. F. Chabalowski, M. J. Frisch, *J. Phys. Chem.* **1994**, *98*, 11623–11627; e) S. H. Volko, L. Wilk, M. Nusair, *Can. J. Phys.* **1980**, *58*, 1200–1211.

[14] Y. Zhao, D. G. Truhlar, *Acc. Chem. Res.* **2008**, *41*, 157–167.

[15] D. Andrae, U. Haeussermann, M. Dolg, H. Stoll, H. Preuss, *Theor. Chim. Acta* **1990**, *77*, 123–141.

[16] a) S. Ehrlich, J. Moellmann, S. Grimme, *Acc. Chem. Res.* **2013**, *46*, 916–926; b) J. Antony, R. Sure, S. Grimme, *Chem. Commun.* **2015**, *51*, 1764–1774.

[17] F. Weigend, F. Furche, R. Ahlrichs, *J. Chem. Phys.* **2003**, *119*, 12753–12762.

[18] a) C. P. Kelly, C. J. Cramer, D. G. Truhlar, *J. Phys. Chem. B.* **2006**, *110*, 16066–16081; b) C. P. Kelly, C. J. Cramer, D. G. Truhlar, *J. Phys. Chem. B.* **2007**, *111*, 408–422.

[19] E. D. Glendening, J. K. Badenhoop, A. E. Reed, J. E. Carpenter, J. A. Bohmann, C. M. Morales, P. Karafiloglou, C. R. Landis, F. Weinhold, *NBO 7.0.*, Theoretical Chemistry Institute, University of Wisconsin–Madison (USA), **2018**.

[20] A. Bondi, *J. Phys. Chem.* **1964**, *68*, 441–451.

[21] a) J. F. Hartwig, K. S. Cook, M. Hapke, C. D. Incarvito, Y. Fan, C. E. Webster, M. B. Hall, *J. Am. Chem. Soc.* **2005**, *127*, 2538–2552; b) C. S. Wei, C. A. Jiménez-Hoyos, M. F. Videa, J. F. Hartwig, M. B. Hall, *J. Am. Chem. Soc.* **2010**, *132*, 3078–3091.

[22] A. J. Canty, R. T. Honeyman, B. W. Skelton, A. H. White, *Acta Crystallogr. Sect. C* **2004**, *60*, o98-o99.

[23] G. Desiraju, P. S. Ho, L. Kloo, A. C. Legon, R. Marquardt, P. Metrangolo, P. Politzer, G. Resnatj, K. Rissanen, *Pure Appl. Chem.* **2013**, *85*, 1711–1713.

[24] a) M. H. P. Rietveld, D. M. Grove, G. van Koten, *New J. Chem.* **1997**, *21*, 751–771; b) J.-P. Pascal, S. L. James, P. Steenwinkel, T. Karlen, D. M. Grove, N. Veldman, W. J. J. Smeets, A. L. Spek, G. van Koten, *Organometallics* **1996**, *15*, 941–948.

[25] a) M. P. Brown, R. J. Puddephatt, C. E. E. Upton, *J. Chem. Soc. Dalton Trans.* **1974**, 2457–2465; b) K. I. Goldberg, J. Yan, E. M. Breitung, *J. Am. Chem. Soc.* **1995**, *117*, 6889–6896; c) D. M. Crumpton, K. I. Goldberg, *J. Am. Chem. Soc.* **2000**, *122*, 962–963; d) D. M. Crumpton-Bregel, K. I. Goldberg, *J. Am. Chem. Soc.* **2003**, *125*, 9442–9458; e) J. Procelewska, A. Zahl, G. Liehr, R. van Eldik, N. A. Smythe, B. S. Williams, K. I. Goldberg, *Inorg. Chem.* **2005**, *44*, 7732–7742; f) C. Gallego, M. Martinez, V. Sixte Safont, *Organometallics* **2007**, *26*, 527–537; g) C. Michel, A. Laio, F. Mohamed, M. Krack, M. Parrinello, A. Milet, *Organometallics* **2007**, *26*, 1241–249; h) A. Yahav-Levi, I. Goldberg, A. Vigalok, A. N. Vedernikov, *J. Am. Chem. Soc.* **2008**, *130*, 724–731; i) A. Ariafard, Z. Ejehi, H. Sadrara, T. Mehrabi, S. Etaati, A. Moradzadeh, M. Moshtaghi, H. Nosrati, N. J Brookes, B. F. Yates, *Organometallics* **2011**, *30*, 422–432; j) M. P. Lanci, M. S. Remy, D. B. Lao, M. S. Sanford, J. M. Mayer, *Organometallics* **2011**, *30*, 3704–3707; k) A. Vigalok, *Acc. Chem. Res.* **2015**, *48*, 238–247; l) P. A. Shaw, J. P. Rourke, *Dalton Trans.* **2017**, *46*, 4768–4776; m) F. N. Hosseini, S. M. Nabavizadeh, R. Shoara, M. D. Aseman, M. M. Abu-Omar, *Organometallics* **2021**, *40*, 2051–2063.

[26] a) P. S. Braterman, *J. Chem. Soc. Chem. Commun.* **1979**, 70–71; b) P. S. Braterman, *Top. Curr. Chem.* **1980**, *92*, 149–172.

Manuscript received: July 22, 2021
Accepted manuscript online: September 2, 2021
Version of record online: October 8, 2021

